

# Mutation of a Highly Conserved Aspartic Acid in the $\beta_2$ Adrenergic Receptor: Constitutive Activation, Structural Instability, and Conformational Rearrangement of Transmembrane Segment 6

SØREN G.F. RASMUSSEN, ANNE D. JENSEN, GEORGE LIAPAKIS, PEJMAN GHANOUNI, JONATHAN A. JAVITCH, and ULRIK GETHER

*Division of Cellular and Molecular Physiology, Department of Medical Physiology 12.5, The Panum Institute, University of Copenhagen, Copenhagen, Denmark (S.G.F.R., A.D.J., P.G., U.G.); and Center for Molecular Recognition, Columbia University College of Physicians and Surgeons, New York, New York (G.L., J.A.J.)*

Received January 27, 1999; accepted April 20, 1999

This paper is available online at <http://www.molpharm.org>

## ABSTRACT

Movements of transmembrane segments (TMs) 3 and 6 play a key role in activation of G protein-coupled receptors. However, the underlying molecular processes that govern these movements, and accordingly control receptor activation, remain unclear. To elucidate the importance of the conserved aspartic acid (Asp-130) in the Asp-Arg-Tyr motif of the  $\beta_2$  adrenergic receptor ( $\beta_2$ AR), we mutated this residue to asparagine (D130N) to mimic its protonated state, and to alanine (D130A) to fully remove the functionality of the side chain. Both mutants displayed evidence of constitutive receptor activation. In COS-7 cells expressing either D130N or D130A, basal levels of cAMP accumulation were clearly elevated compared with cells expressing the wild-type  $\beta_2$ AR. Incubation of COS-7 cell membranes or purified receptor at 37°C revealed also a marked

structural instability of both mutant receptors, suggesting that stabilizing intramolecular constraints had been disrupted. Moreover, we obtained evidence for a conformational rearrangement by mutation of Asp-130. In D130N, a cysteine in TM 6, Cys-285, which is not accessible in the wild-type  $\beta_2$ AR, became accessible to methanethiosulfonate ethylammonium, a charged, sulfhydryl-reactive reagent. This is consistent with a counterclockwise rotation or tilting of TM 6 and provides for the first time structural evidence linking charge-neutralizing mutations of the aspartic acid in the DRY motif to the overall conformational state of the receptor. We propose that protonation of the aspartic acid leads to release of constraining intramolecular interactions, resulting in movements of TM 6 and, thus, conversion of the receptor to the active state.

The majority of hormones and neurotransmitters exert their cellular effects by binding to cell surface receptors belonging to the superfamily of G protein-coupled receptors (GPCRs; Strader et al., 1994; Gether and Kobilka, 1998; Ji et al., 1998). The  $\beta_2$  adrenergic receptor ( $\beta_2$ AR) belongs to the subfamily of rhodopsin-like receptors and has been used as a prototype GPCR in numerous studies (Gether and Kobilka, 1998; Strader et al., 1994). Structurally, GPCRs are characterized by the presence of seven membrane-spanning  $\alpha$ -heli-

cal segments. High resolution structural information is not yet available due to the inherent difficulties in purifying and crystallizing large membrane proteins (Gether and Kobilka, 1998; Ji et al., 1998). Nevertheless, the low-resolution structure of rhodopsin, resolved by Schertler and coworkers (1993; Unger et al., 1997), has provided important insight into the organization of the seven-helix bundle and allowed development of tertiary structure models of the receptors (Balles-teros and Weinstein, 1995; Scheer et al., 1996; Baldwin et al., 1997).

A fundamental question in understanding the function of GPCRs at a molecular level is how agonist binding to the receptor is converted into receptor activation (Gether and Kobilka, 1998). Only recently, techniques have been established that permit direct structural analyses of conformational changes accompanying receptor activation. Khorana,

The study was supported in part by the Danish Natural Science Research Council, the Danish Cancer Society, the Danish Heart Foundation, and the NOVO Nordisk Foundation. U.G. is the recipient of an Ole Rømer Associate Research Professorship from the Danish Natural Science Research Council. In addition, this work was supported in part by National Institutes of Health Grants MH57324 and MH54137, by the G. Harold & Leila Y. Mathers Charitable Trust, and by the Lebovitz Trust (J.A.J.).

**ABBREVIATIONS:** GPCR, G protein-coupled receptor;  $\beta_2$ AR,  $\beta_2$  adrenergic receptor; TM, transmembrane segment; MTSEA, methanethiosulfonate ethylammonium; WT, wild-type; ISO, isoproterenol; DRY, Asp-Arg-Tyr; GnRH, gonadotropin-releasing hormone; Asp-130, aspartic acid in the DRY motif of the human  $\beta_2$ AR; MTS, methanethiosulfonate; PCR, polymerase chain reaction; EPR, electron paramagnetic resonance; CAM, the constitutively activated  $\beta_2$ AR mutant L266S/K267R/H269K/L272A; HEK, human embryonic kidney.

Hubble, and coworkers have used electron paramagnetic resonance (EPR) spectroscopy to study conformational changes accompanying photoactivation of rhodopsin (Farrens et al., 1996). Using site-selective incorporation of pairs of sulfhydryl-reactive spin labels, they have demonstrated that photoactivation of rhodopsin involves rigid-body movement of transmembrane segment (TM) 6 relative to TM 3 (Farrens et al., 1996). Gether et al. (1995, 1997a,b) have analyzed ligand-induced conformational changes in the  $\beta$ 2AR using fluorescence spectroscopy analysis of purified  $\beta$ 2AR cysteine mutants, which were site-selectively labeled with a sulfhydryl-reactive and environmentally sensitive fluorophore. In agreement with the rhodopsin data, it was found that agonist-promoted activation involves critical movements of TMs 3 and 6 (Gether et al., 1997b). A key role of these domains has been supported further by the observation that bis-His  $\text{Zn}^{2+}$  binding sites and disulfide cross-links generated between TMs 3 and 6 prevent receptor activation and G protein coupling (Yu et al., 1995; Sheikh et al., 1996). The molecular mechanisms, however, that underlie the movements of TMs 3 and 6, and thus govern the transition of the receptor between its inactive and active state, remain unclear.

It has been suggested that receptor activation involves protonation of the aspartic acid in the conserved Asp-Arg-Tyr (DRY) motif at the cytoplasmic side of TM 3 (Fig. 1; Scheer et al., 1996, 1997). Charge-neutralizing mutations of the aspartic acid lead to increased agonist-independent activity of the

$\alpha_{1b}$ -adrenergic receptor (Scheer et al., 1996, 1997) and more efficient coupling of the gonadotropin-releasing hormone (GnRH) receptor (Ballesteros et al., 1998). In rhodopsin, mutation of the corresponding glutamic acid also causes weak constitutive receptor activation (Cohen et al., 1993). In addition, experiments have indicated that the glutamic acid is partly responsible for the proton uptake that has been shown to accompany formation of the activated metarhodopsin II intermediate (Arnis et al., 1994). Therefore, we hypothesized that the aspartic acid of the DRY motif in its unprotonated state forms stabilizing intramolecular interactions that restrain movements of TMs 3 and 6, thus maintaining the receptor in an inactive configuration.

To test this hypothesis the aspartic acid in the DRY motif of the human  $\beta$ 2AR (Asp-130; Asp3.49 according to the general nomenclature proposed in Ballesteros and Weinstein, 1995) was mutated to asparagine (D130N) to mimic the protonated state of the side chain and alanine (D130A) to completely remove its functionality. Our hypothesis was supported by the observations that mutation of Asp-130 leads to constitutive receptor activation and a marked structural instability of the receptor protein. Moreover, we obtained evidence that mimicking the protonated state of Asp-130 in TM 3 leads to a conformational rearrangement in TM 6 consistent with a counterclockwise rotation (as seen from the extracellular side) or tilting of the helix. We suggest that Asp-130 is an important part of a molecular switch that controls transition of the receptor between its active and inactive state and thus may govern the spatial disposition of TMs 3 and 6.

## Experimental Procedures

**Site-Directed Mutagenesis.** The mutations of Asp-130 to D130N and D130A in the  $\beta$ 2AR were generated by polymerase chain reaction (PCR)-mediated mutagenesis using the Pfu polymerase according to the manufacturer's instructions (Stratagene, La Jolla, CA). The mutation of Cys-285 (C285S) was generated as described (Javitch et al., 1997). The constitutively activated  $\beta$ 2AR mutant, CAM (L266S/K267R/H269K/L272A), was provided by Dr. R. J. Lefkowitz (Duke University, Durham, NC). The DNA fragments containing the Asp-130 mutations or CAM were cloned into an epitope-tagged version of the human  $\beta$ 2AR (Sf-h $\beta$ 2-6H; Guan et al., 1992; Gether et al., 1997b) in the mammalian expression vectors pcDNA3 (Stratagene, La Jolla, CA) and pTEJ8 (Johansen et al., 1990). For expression in Sf-9 insect cells the mutants were cloned into the baculovirus expression vector pVL1392 (Invitrogen, San Diego, CA). For transient expression in HEK-293 cells, the wild-type (WT) receptor, D130N, and D130N/C285S were cloned into pCIN4 (Javitch et al., 1997). The mutations were identified initially through the presence of diagnostic restriction sites introduced via the mutated oligonucleotides, and subsequently verified by DNA sequencing analysis of the PCR-generated segments.

**Cell Culture and Transfection.** COS-7 cells were grown at 37°C in 10%  $\text{CO}_2$  in Dulbecco's modified Eagle's medium 1885, supplemented with 10% fetal calf serum, 2 mM glutamine, and 0.01 mg/ml gentamycin. For transient expression, COS-7 cells were transfected by the calcium phosphate precipitation method (Johansen et al., 1990) using 10 to 60  $\mu\text{g}$  of the pcDNA3 or pTEJ-8 constructs per  $6 \times 10^6$  cells in 175  $\text{cm}^2$  flasks. The amount of DNA used in the transfections was modified to achieve various expression levels of the constructs. Human embryonic kidney (HEK) 293 cells were maintained at 37°C in 5%  $\text{CO}_2$  in Dulbecco's modified Eagle's medium/F-12 (1:1), containing 3.15 g/liter glucose in 10% fetal calf serum. The HEK 293 cells were transiently transfected with 2  $\mu\text{g}$  DNA of the

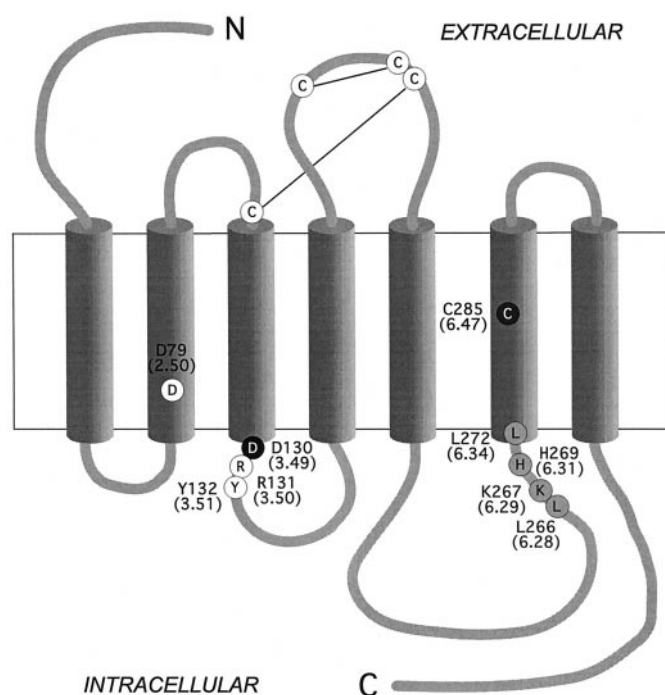


**Fig. 1.** Two-dimensional model of the  $\beta$ 2AR. The highly conserved DRY motif is located at the cytoplasmic side of TM 3. The conserved aspartic acid Asp-130<sup>3.49</sup> is indicated with a white letter in a black circle whereas Arg-131<sup>3.50</sup> and Tyr-132<sup>3.51</sup> are shown with a black letter in a white circle. The cysteine (Cys-285<sup>6.47</sup>) that becomes partially accessible in the D130N mutant and in CAM (Javitch et al., 1997) is located in TM 6 and is indicated with a white letter in a dark shaded circle. The four residues mutated in CAM (Samama et al., 1993) are indicated with black letters in light shaded circles. The highly conserved aspartic acid in TM 2 (Asp-79<sup>2.50</sup>) are shown with black letters in white circles. The numbers in parentheses (or superscript) refer to the general numbering scheme for GPCRs proposed in Ballesteros and Weinstein, 1995.

pCIN4 constructs using the Lipofectamine/Opti-MEM (Life Technologies, Inc., Grand Island, NY) transfection system as described (Javitch et al., 1997). Sf-9 cells were grown in suspension culture in SF 900II medium (Gibco, Grand Island, NY) containing 5% fetal calf serum and 0.1 mg/ml gentamycin (Gibco). Expressions in Sf-9 insect cells were obtained by cotransfection of the pVL1392 constructs with linearized BaculoGold DNA using the BaculoGold transfection kit (Pharmingen, San Diego, CA). The resulting recombinant viruses were amplified to high titer stocks as described (Gether et al., 1997b; U.G., in press).

**COS-7 Cell Membrane Preparation.** Membranes were prepared from transiently transfected COS-7 cells 48 h post-transfection. The cells were washed once with PBS (8.1 mM  $\text{NaH}_2\text{PO}_4$ , 1.5 mM  $\text{KH}_2\text{PO}_4$ , 138 mM NaCl, 2.7 mM KCl, pH 7.2) before addition of 10 ml of ice-cold lysis buffer per  $10^7$  cells in a 175  $\text{cm}^2$  flask (10 mM Tris-HCl, pH 7.5, containing 1 mM EDTA, 10  $\mu\text{g}/\text{ml}$  of the protease inhibitors benzamidine and leupeptin, plus 0.5 mM phenylmethylsulfonyl fluoride). The cells were detached in the lysis buffer by scraping with a cell scraper and homogenized in a Dounce homogenizer (25 strokes with the tight pestle). The lysed cells were centrifuged for 5 min at 500g, and the resulting supernatant was centrifuged at 40,000g for 30 min at 4°C. The membrane pellet was resuspended in ice-cold binding buffer (75 mM Tris-HCl, pH 7.4, 12.5 mM  $\text{MgCl}_2$ , 1 mM EDTA) containing the above mentioned protease inhibitors. Protein was determined using the Bio-Rad DC protein assay kit (Bio-Rad, Richmond, CA). Membranes were diluted to 1 mg protein/ml in binding buffer before storage at -80°C.

**Ligand Binding.** In saturation-binding experiments, COS-7 cell membranes (5–50  $\mu\text{g}$  membrane protein) were incubated for 2 h at room temperature with  $10^{-11}$  to  $10^{-8}$  M [ $^3\text{H}$ ]dihydroalprenolol (TRK 649; Amersham, Little Chalfont, UK) in a total volume of 500  $\mu\text{l}$  binding buffer (75 mM Tris-HCl, pH 7.4, 12.5 mM  $\text{MgCl}_2$ , 1 mM EDTA). Nonspecific binding was determined in presence of 10  $\mu\text{M}$  alprenolol. In competition binding experiments, membrane protein (between 5 and 50  $\mu\text{g}$  depending on the receptor expression) was incubated for 2 h at room temperature with 0.5 nM [ $^3\text{H}$ ]dihydroalprenolol and increasing concentration of isoproterenol (ISO) or pindolol. All determinations in the binding assays were done in triplicate. The binding reactions were stopped by rapid filtration over glass fiber filters (FilterMat B, Wallac, Turku, Finland) using a 96-well Tomtec cell harvester (Tomtec, Hamden, CT). MeltiLex Melt-on Scintillator Sheets (Wallac) were used for counting of the filter in a Wallac Tri-Lux  $\beta$  scintillation counter.  $K_d$  and  $\text{IC}_{50}$  values were determined by nonlinear regression analysis using GraphPad Prism 2.0 (GraphPad Software, San Diego, CA).  $K_i$  values were determined using the equation  $K_i = \text{IC}_{50}/(1 + L/K_d)$ .

**cAMP Accumulation Assay.** The cAMP accumulation assay was performed essentially as described (Salomon et al., 1974; Hjorth et al., 1998). COS-7 cells, transiently expressing the WT and mutant receptors, were cultured in 12-well plates ( $2.5 \times 10^5$  cells/well) and incubated overnight with medium containing 2  $\mu\text{Ci}/\text{ml}$  of [ $^3\text{H}$ ]adenine (TRK311, Amersham). The cells were washed twice in 1.0 ml HBS buffer (25 mM HEPES pH 7.2, 0.75 mM  $\text{NaH}_2\text{PO}_4$ , 140 mM NaCl) followed by incubation for 20 min at 37°C in the absence or presence of ligand in 1.0 ml of HBS containing 1.0 mM 3-isobutyl-1-methylxanthine. The cells were chilled on ice, the incubation mix was aspirated, and the incubations were terminated by adding 1.0 ml of ice-cold 5% trichloroacetic acid containing 0.1 mM unlabeled cAMP and ATP. After 30 min on ice, the supernatants were applied first to a Bio-Rad 50W-X4 resin and subsequently to an alumina column (Sigma, St. Louis, MO). The [ $^3\text{H}$ ]cAMP generated was eluted into scintillation tubes in 0.1 M imidazole, after which scintillation fluid was added and the samples counted. Determination of basal activity was performed in quadruplicate, ligand-stimulated activity in duplicate. In each experiment, the expression of the receptor constructs was assessed in a binding assay, performed as described above, using a single saturating concentration of [ $^3\text{H}$ ]dihydroalprenolol (10 nM). Crude membranes were prepared for the binding

assay from  $1.5 \times 10^6$  cells grown overnight in 10-cm tissue culture dishes.

**Sf-9 Membrane Preparation and Adenylyl Cyclase Assay.** Sf-9 cells (25-ml cultures in 125-ml disposable Erlenmeyer flasks at a density of  $3 \times 10^6$  cells/ml) were infected with baculovirus encoding the WT or mutant receptors for 24 to 64 h. The incubation time was varied to obtain similar levels of expression for the individual receptor constructs. The cells were harvested and membranes prepared according to previously described procedures (Gether et al., 1995). Adenylyl cyclase assay was performed on the membranes as described (Suryanarayana and Kobilka, 1991).

**Assessment of Receptor Stability in Membranes.** COS-7 cell membranes (1 mg protein/ml) expressing WT or mutant receptors were diluted 4-fold in binding buffer containing 10  $\mu\text{g}/\text{ml}$  of the protease inhibitors benzamidine and leupeptin plus 0.5 mM phenylmethylsulfonyl fluoride. The membranes were subsequently incubated for 0 (control), 2, 6, 12, and 24 h at 37°C. The remaining binding activity was assessed in a binding assay performed as described above using a single saturating concentration of [ $^3\text{H}$ ]dihydroalprenolol (10 nM). To assess the ability of ligands to affect receptor stability, membranes expressing the WT or the D130A mutant were incubated for 6 h at 37°C in binding buffer containing protease inhibitors plus 10  $\mu\text{M}$  (–)-ISO with 10 mM ascorbate or 1  $\mu\text{M}$  ICI 118,551. Before performing the binding assay, the membranes were washed twice in binding buffer with protease inhibitors by pelleting the membranes at 15,000g for 20 min, followed by resuspension in equal volumes of ice-cold buffer.

**Assessment of Stability of Purified Receptor.** For nickel-purification of the WT and the D130A mutant, Sf-9 cells were grown in 500-ml cultures at a density of  $3 \times 10^6$  cells/ml, infected with a 1:30 dilution of a high titer virus stock and harvested after 48 h. The receptors were solubilized in 1.0% (w/v) *n*-dodecyl- $\beta$ -D-maltoside (Anatrace, Maumee, OH) and purified by nickel-column chromatography using Chelating Sepharose (Amersham Pharmacia Biotech AB, Uppsala, Sweden) as described (U.G., in press). Stability of the nickel-purified receptor was determined by incubating 2 pmol receptor at 37°C for 0, 15, 30, and 60 min in 20 mM Tris-HCl, pH 7.5, containing 0.08% (w/v) *n*-dodecyl- $\beta$ -D-maltoside, 100 mM NaCl, and 5 mg/ml bovine serum albumin. The remaining binding activity of the receptors was assessed in a binding assay using a single saturating concentration of [ $^3\text{H}$ ]dihydroalprenolol (10 nM) as described (Gether et al., 1997b). Purified receptor incubated for 0 and 60 min at 37°C was analyzed by 10% SDS-polyacrylamide gel electrophoresis followed by Western blotting using the M1 antiFLAG antibody (Sigma Chemical Co., St. Louis, MO) and the enhanced chemiluminescence system (Pierce, Rockford, IL).

**Methanethiosulfonate (MTS) Reagent Assay.** The MTS reagent assay was carried out as described (Javitch et al., 1994, 1997). The HEK 293 cells, grown in 35-mm dishes and transiently expressing the D130N or the D130N/C285S mutants, were washed in PBS, briefly treated with PBS containing 5 mM EDTA, and then dissociated in PBS. Cells were pelleted at 1000g for 5 min at 4°C and resuspended in 400  $\mu\text{l}$  of buffer (140 mM NaCl, 5.4 mM KCl, 1 mM EDTA, 0.006% BSA, 25 mM HEPES, pH 7.4). Aliquots of whole-cell suspension (50  $\mu\text{l}$ ) were incubated with different concentrations of freshly prepared methanethiosulfonate ethylammonium (MTSEA; Toronto Research Biochemicals) for 2 min at room temperature. Cell suspensions were diluted 20-fold and binding of [ $^3\text{H}$ ]CGP-12177 (400–800 pM) was measured on 300  $\mu\text{l}$  aliquots in triplicate using 1  $\mu\text{M}$  alprenolol to determine nonspecific binding. Fractional inhibition was calculated as  $1 - [(\text{specific binding after MTS reagent})/(\text{specific binding without reagent})]$ .

## Results

**Constitutive Activation of  $\beta_2\text{AR}$  by Mutation of Asp-130.** The aspartic acid in the conserved DRY-motif of the  $\beta_2\text{AR}$  (Asp-130<sup>3,49</sup>, see Fig. 1) was mutated to asparagine



and alanine (D130N and D130A). As illustrated in Fig. 2, these charge-neutralizing mutations caused a clear elevation of basal, agonist-independent cAMP accumulation in transiently transfected COS-7 cells as compared with the WT receptor. The basal activity increased linearly with increasing receptor expression. D130N displayed the highest activity (slope =  $0.31 \times 10^3$  cpm  $\times$  pmol $^{-1}$   $\times$  mg protein $^{-1}$ ) followed by D130A (slope =  $0.174 \times 10^3$  cpm  $\times$  pmol $^{-1}$   $\times$  mg protein $^{-1}$ ) and WT (slope =  $0.013 \times 10^3$  cpm  $\times$  pmol $^{-1}$   $\times$  mg protein $^{-1}$ ; Fig. 2). The activity of the mutants was compared to CAM (Samama et al., 1993), which contains four substitutions at the cytoplasmic side of TM 6 (L266S/K267R/H269K/L272A; Fig. 1). CAM displayed a basal activity simi-

lar to D130A (slope =  $0.175 \times 10^3$  cpm  $\times$  pmol $^{-1}$   $\times$  mg protein $^{-1}$ ; Fig. 2).

Stimulation of COS-7 cells transiently expressing the WT or mutant receptors with a saturating concentration of the partial agonist pindolol (1  $\mu$ M) caused a clear increase in cAMP accumulation that increased with increasing expression of the individual receptor constructs (Fig. 3). As observed for the basal activity, the increase in cAMP accumulation was most significant for D130N (slope =  $2.1 \times 10^3$  cpm  $\times$  pmol $^{-1}$   $\times$  mg protein $^{-1}$ ) followed by D130A (slope =  $0.81 \times 10^3$  cpm  $\times$  pmol $^{-1}$   $\times$  mg protein $^{-1}$ ), CAM (slope =  $0.76 \times 10^3$  cpm  $\times$  pmol $^{-1}$   $\times$  mg protein $^{-1}$ ), and WT (slope =  $0.129 \times 10^3$  cpm  $\times$  pmol $^{-1}$   $\times$  mg protein $^{-1}$ ; Fig. 3).

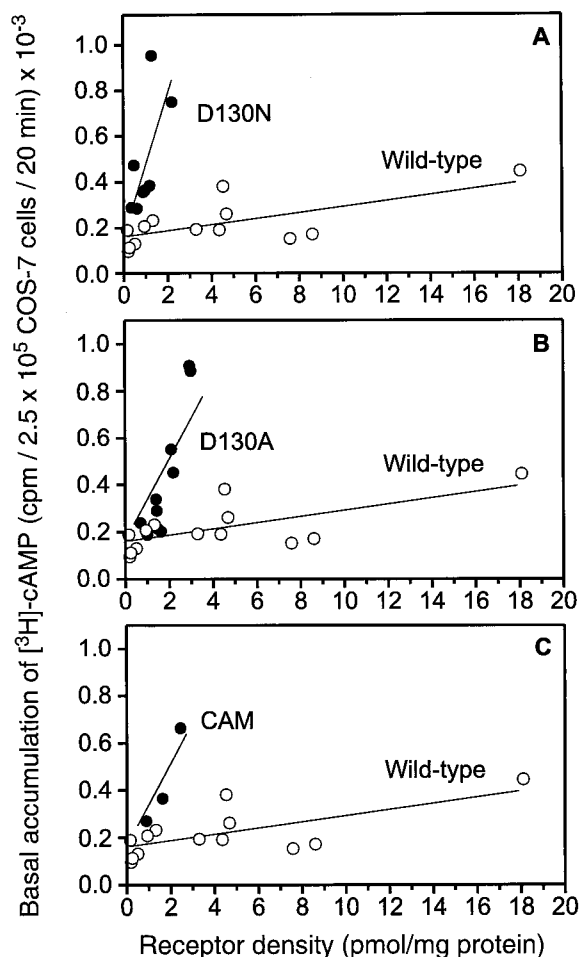


**Fig. 2.** Evidence for constitutive activation of D130A, D130N, and CAM. A, basal [ $^3$ H]cAMP accumulation in COS-7 cells transiently expressing D130N (●) or WT  $\beta$ 2AR (○). B, basal [ $^3$ H]cAMP accumulation in COS-7 cells transiently expressing D130A (●) or WT  $\beta$ 2AR (○). C, basal [ $^3$ H]cAMP accumulation in COS-7 cells, transiently expressing CAM (●) or WT  $\beta$ 2AR (○). The values are plotted as a function of receptor density, and are obtained from  $n = 13, 8, 10$ , and 3 individual transfections of WT, D130N, D130A, and CAM, respectively. To obtain a series of different expression levels of the WT, DNA used in the transfections was varied between 10 and 60  $\mu$ g. Each determination was done in quadruplicate. The lines shown were calculated by linear regression analysis with the lines forced through the y axis corresponding to the measured [ $^3$ H]cAMP accumulation in nontransfected COS-7 cells. The slopes of the lines are as follows: WT,  $0.013 \times 10^3$  cpm  $\times$  pmol $^{-1}$   $\times$  mg protein $^{-1}$ ; D130N,  $0.31 \times 10^3$  cpm  $\times$  pmol $^{-1}$   $\times$  mg protein $^{-1}$ ; D130A,  $0.174 \times 10^3$  cpm  $\times$  pmol $^{-1}$   $\times$  mg protein $^{-1}$ ; CAM,  $0.175 \times 10^3$  cpm  $\times$  pmol $^{-1}$   $\times$  mg protein $^{-1}$ .

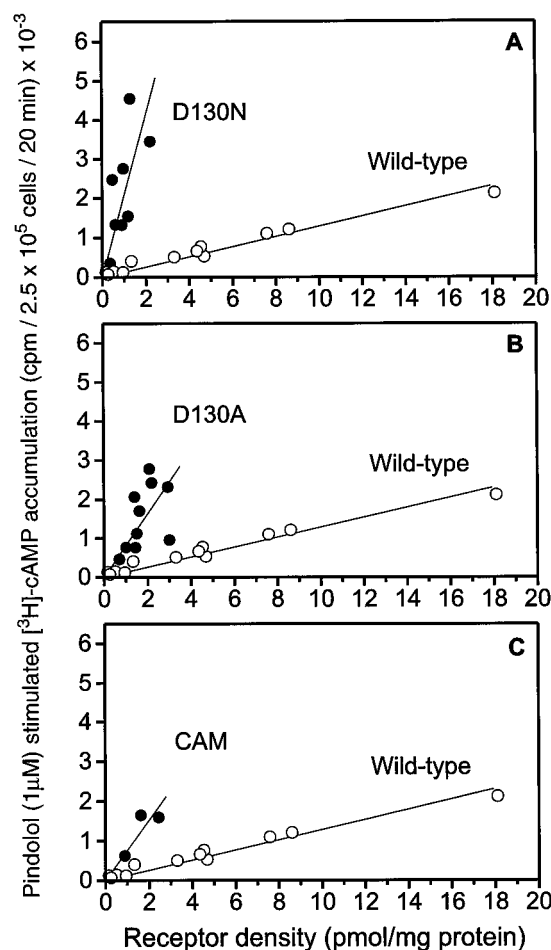


**Fig. 3.** Increased response to pindolol at D130A, D130N, and CAM. A, pindolol-stimulated increase in [ $^3$ H]cAMP accumulation in COS-7 cells transiently expressing D130N (●) or WT  $\beta$ 2AR (○). B, pindolol-stimulated increase in [ $^3$ H]cAMP accumulation in COS-7 cells transiently expressing D130A (●) or WT  $\beta$ 2AR (○). C, pindolol-stimulated increase in [ $^3$ H]cAMP accumulation in COS-7 cells transiently expressing CAM (●) or WT  $\beta$ 2AR (○). Data are expressed as the difference between basal activity in the absence of pindolol and the activity in the presence of 1  $\mu$ M pindolol. The values are plotted as a function of receptor density and are obtained from  $n = 13, 8, 10$ , and 3 individual transfections of WT, D130N, D130A, and CAM, respectively. To obtain a series of different expression levels of the WT, the DNA used in the transfections was varied between 10 and 60  $\mu$ g. Each determination was done in duplicate. The lines shown were calculated by linear regression analysis. The slopes of the lines are as follows: WT,  $0.129 \times 10^3$  cpm  $\times$  pmol $^{-1}$   $\times$  mg protein $^{-1}$ ; D130N,  $2.1 \times 10^3$  cpm  $\times$  pmol $^{-1}$   $\times$  mg protein $^{-1}$ ; D130A,  $0.81 \times 10^3$  cpm  $\times$  pmol $^{-1}$   $\times$  mg protein $^{-1}$ ; CAM,  $0.76 \times 10^3$  cpm  $\times$  pmol $^{-1}$   $\times$  mg protein $^{-1}$ .

The data indicate an increased efficacy of pindolol at all three mutant receptors. Increased efficacy of partial agonists has previously been described for CAM and is consistent with an enhanced ability of the mutant receptors to assume an activated state (Samama et al., 1993). Because ISO significantly increased cAMP levels in untransfected COS-7 cells by stimulating endogenous  $\beta_2$ ARs present at low levels (data not shown), it was not possible to investigate the response of the mutant receptors to full agonists. The partial agonist, pindolol, however, did not affect cAMP production in untransfected cells (data not shown).

Pindolol dose-response curves at D130N, D130A, and WT revealed a 4- to 5-fold increase in potency of pindolol at D130N and D130A in stimulating cAMP production (Fig. 4). Notably, increased potency for partial agonists has been described previously for CAM (Samama et al., 1993).

#### Expression of D130N and D130A in Sf-9 Insect Cells.

To assess maximum receptor activity of the mutants (response to full agonists) and to confirm our observations in COS-7 cells, the WT receptor, D130N, and D130A were expressed in Sf-9 insect cells, which do not contain endogenous  $\beta$  adrenergic receptors (Chidiac et al., 1994). Unfortunately,

the expression of the D130N mutant in the Sf-9 insect cells was too low for functional studies. However, the D130A mutant was expressed at levels allowing measurements of coupling to adenylyl cyclase. In agreement with our observations in COS-7 cells, adenylyl cyclase assays on Sf-9 cell membranes showed higher basal adenylyl cyclase activity for D130A than for the WT receptor at similar expression levels (Fig. 5). Moreover, we observed an increased potency of the full agonist, ISO and an increased maximum response at D130A as compared with the WT (Fig. 5). These data suggest that mutation of Asp-130 causes both constitutive activation and receptor hyperactivity.

In the Sf-9 insect cell membranes, expressing around 0.8 pmol receptor/mg protein, pindolol behaved as a neutral antagonist at the D130A mutant (maximal response was less than 5% of maximum ISO response) and as a weak inverse agonist at the WT (data not shown). This low efficacy of pindolol is in full agreement with previous observations showing general low efficacy of weak partial agonists in adenylyl cyclase assays on Sf-9 cell membranes as compared with cAMP accumulation measurements on intact cells (Samama et al., 1993; Chidiac et al., 1994).

**Binding Characteristics of Mutant Receptors.** Saturation binding experiments with the antagonist [ $^3$ H]dihydroalprenolol showed unchanged antagonist affinity for all three mutants (D130N, D130A, and CAM) as compared with the WT (Table 1). Receptor expression was, however, markedly reduced, particularly for D130N (Table 1). Expression of the endogenous  $\beta$  adrenergic receptor was less than 100 fmol/mg protein and therefore should not interfere with our binding measurements on the transfected receptors, all of which expressed at levels at least 10-fold higher.

ISO competition binding on COS-7 cell membranes expressing the WT  $\beta_2$ AR revealed a single binding site (Hill slope  $\approx 1$ ) with a  $K_i$  value of 281 nM (Table 2 and Fig. 6). GTP $\gamma$ S treatment did not affect the ISO affinity or the slope of the binding curve (Fig. 6 and Table 2), suggesting that only a negligible fraction of the WT receptors is coupled to G

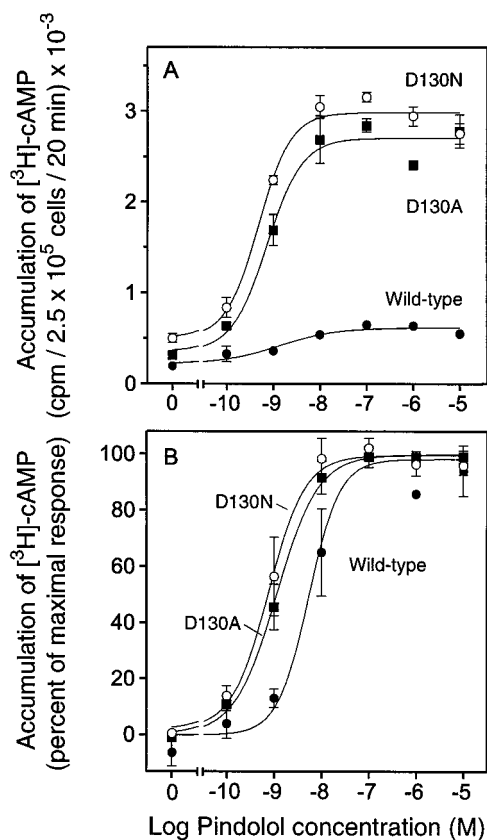


**Fig. 4.** Pindolol dose-response curves of cAMP accumulation in COS-7 cells transiently expressing the WT, D130N, or D130A. A, accumulation of [ $^3$ H]cAMP in response to indicated concentrations of pindolol in COS-7 cells expressing the WT receptor (●), D130N (○), or D130A (■). Data are mean  $\pm$  S.E. of duplicate determinations in a representative experiment. The cells expressed 1.33 pmol/mg, 0.47 pmol/mg, or 1.41 pmol/mg membrane protein of either WT, D130N, or D130A, respectively. The similar levels of expression were achieved by adjusting the DNA used in the transfections. B, dose-response curves from A are given as the percentage of maximum pindolol activity. Maximum pindolol activity was assessed from the dose-response curves by nonlinear regression analysis using Prism (GraphPad, San Diego, CA).

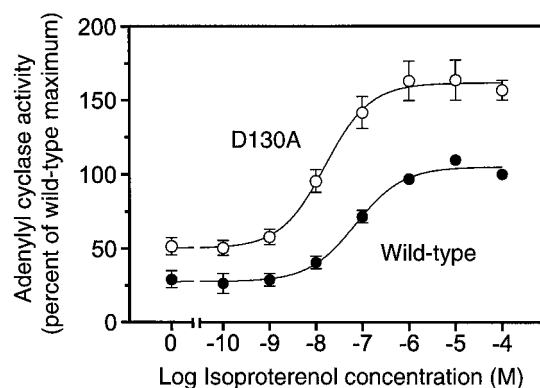


**Fig. 5.** Adenylyl cyclase activity in membranes from Sf-9 insect cells expressing the WT  $\beta_2$ AR or D130A. ISO dose-response of adenylyl cyclase activity in membranes expressing either the WT receptor (●) or D130A (○). Data are given as the percentage of maximum ISO-stimulated adenylyl cyclase activity of the WT and are expressed as mean  $\pm$  S.E. of four different experiments. Maximum activity of the WT was 11.6 pmol cAMP/mg protein/min and assessed from the dose-response curves by nonlinear regression analysis using Prism (GraphPad). The membrane preparations used contained 0.81 pmol WT receptor/mg protein or 0.79 pmol D130A pmol/mg protein. The similar levels of expression were achieved by shortening the incubation time to 24 h for the WT after infection with virus.

protein and thus forms the high-affinity ternary complex (Samama et al., 1993). Notably, similar results were obtained over a wide range of expression levels (from 1 pmol receptor/mg protein to 10 pmol/mg protein; data not shown). In contrast to the WT, the ISO competition curves for D130N, D130A, and CAM showed the best fit to a two-site model (Fig. 6 and Table 2). The  $K_i$  value for the high-affinity site ranged from 0.6 to 1.0 nM whereas the  $K_i$  value for the low-affinity site was 10 to 20 nM (Table 2). The apparent high-affinity site most likely reflected receptors coupled to the G protein because GTP $\gamma$ S treatment of the membranes eliminated the high-affinity site and resulted in monophasic binding curves with a Hill slopes close to unity (Fig. 6 and Table 2). The affinity of ISO for CAM, D130N, and D130A in the presence of GTP $\gamma$ S was similar to the affinity of the low-affinity site detected in the absence of GTP $\gamma$ S (Table 2). However, the affinity of ISO for this presumably uncoupled state was markedly higher in all three mutants (10- to 30-fold) than for the WT receptor (Table 2). Taken together, these data indicate that charge-neutralizing mutations of Asp-130 lead to an increase in apparent agonist affinity for the uncoupled state of the receptor. Furthermore, the data indicate a higher degree of high-affinity ternary complex formation in the mutant receptors, consistent with a higher propensity of the receptors to assume the activated R\* state and thus couple to the G protein (Samama et al., 1993).

Competition binding experiments with pindolol demonstrated unchanged affinities for the mutant receptors as compared with the WT (Table 1). This is consistent with the unchanged affinities observed previously in CAM for weak partial agonists such as pindolol (Samama et al., 1993).

**Structural Instability of Asp-130 Mutants.** It has been suggested that the receptor normally is kept quiescent by a

network of constraining intramolecular interactions, and that disruption of such constraints is a key element in constitutive receptor activation (Kjelsberg et al., 1992; Gether et al., 1997a; Gether and Kobilka, 1998). Recently, this hypothesis was supported by the finding that CAM  $\beta$ 2AR is not only constitutively active but is also characterized by a marked structural instability and enhanced conformational flexibility of the purified receptor protein (Gether et al., 1997a). As illustrated in Fig. 7, mutation of Asp-130 also conferred a marked structural instability to the receptor protein. The instability was observed both in situ by incubating COS-7 cell membranes, expressing the different receptors, at 37°C, and by incubating partially purified receptor protein in detergent solution at 37°C. Whereas the  $T_{1/2}$  for degradation of the WT in membranes was 12 to 24 h, the  $T_{1/2}$  values for the mutants were approximately 2.5 h (Fig. 7A). Both the full agonist ISO and the inverse agonist ICI 118,551 were able to stabilize the mutant receptors to a level comparable to the WT (Fig. 7B). The stability of the partially purified receptor protein in detergent solution was much less than that observed for the receptor in membranes (Fig. 7C). However, a clear difference between WT and the D130A mutant was still observable ( $T_{1/2, WT} = 21$  min versus  $T_{1/2, D130A} = 10$  min). Western blot analysis of the partially purified protein after 1 h at 37°C showed no sign of proteolytic degradation (Fig. 7C, inset). Thus, the loss of binding activity apparently reflects denaturation of the protein and not proteolytic degradation.

**Evidence for a Conformational Rearrangement of TM 6.** Treatment of cells expressing the WT  $\beta$ 2AR with up to 100 mM charged, sulfhydryl specific agent, MTSEA, does not affect binding of the radioligand [ $^3$ H]CGP-12177 to the  $\beta$ 2AR (Javitch et al., 1997). However, Javitch et al. (1997) reported recently that high concentrations of MTSEA inhibits binding of [ $^3$ H]CGP-12177 up to around 60% in the constitutively activated mutant CAM (L266S/K267R/H269K/L272A) (Javitch et al., 1997). Mutation of the endogenous cysteine Cys-285 (Cys6.47, see Fig. 1) in TM 6 eliminated the inhibition, suggesting that Cys-285 in CAM becomes partially accessible for MTSEA in the water-accessible binding crevice (Javitch et al., 1997). Because it is reasonable to assume that CAM spontaneously assumes an activated state of the receptor, this change in accessibility most likely reflects a conformational change associated with receptor activation. We therefore decided to assess the conformational state of the D130N mutation by testing the accessibility of Cys-285 to MTSEA. Similar to what was previously observed for CAM

TABLE 1  
Binding properties of WT and mutant  $\beta$ 2ARs

Saturation and competition binding assays were performed on membranes derived from COS-7 cells transiently expressing the WT or mutants' receptors. Values are from three to five independent experiments performed in triplicate. The  $IC_{50}$  values used for calculations of  $K_i$  values were obtained from means of  $pIC_{50}$  values determined by nonlinear regression analysis and the S.E. interval from  $pIC_{50} \pm$  S.E.

Construct	[ $^3$ H]Dihydroalprenolol		Pindolol	
	$K_d \pm$ S.E.	$B_{max} \pm$ S.E.	$K_i$ [S.E. interval]	Hill
	nM	pmol/mg	nM	
WT	0.20 $\pm$ 0.02	14.0 $\pm$ 4.5	0.93[0.892–0.965]	–1.08
D130N	0.22 $\pm$ 0.01	1.0 $\pm$ 0.2	0.92[0.882–0.960]	–1.15
D130A	0.20 $\pm$ 0.02	5.8 $\pm$ 1.0	0.83[0.813–0.851]	–1.01
CAM	0.21 $\pm$ 0.01	5.4 $\pm$ 1.0	0.75[0.708–0.787]	–0.90

TABLE 2  
ISO competition binding in the absence and presence of GTP $\gamma$ S at WT and mutant  $\beta$ 2ARs

Competition binding assays were performed on COS-7 cells membranes with or without 10  $\mu$ M GTP $\gamma$ S using 0.5 nM [ $^3$ H]dihydroalprenolol as radioligand. Values are from three to five independent experiments performed in triplicate. The  $IC_{50}$  values used for calculations of  $K_i$  values were obtained from means of  $pIC_{50}$  values determined by nonlinear regression analysis and the S.E. interval from  $pIC_{50} \pm$  S.E.

Construct	(–)ISO					
	No GTP $\gamma$ S			+10 $\mu$ M GTP $\gamma$ S		
	$K_{i high}$ [S.E. interval]	$K_{i low}$ [S.E. interval]	Fold decrease in $K_{i low}$	Fraction of $K_{i high}$	$K_{i GTP\gamma S}$ [S.E. interval]	Hill $_{GTP\gamma S}$
	nM	nM			nM	
WT	<sup>a</sup>	281 [272.7–289.0] <sup>a</sup>			278 [260.6–295.6]	–1.03
D130N	1.0 [0.65–1.55]	14.0 [10.60–18.47]	20	0.43	11.5 [10.26–12.90]	–1.00
D130A	0.6 [0.27–1.23]	20.5 [17.47–23.97]	14	0.19	22.2 [20.67–23.84]	–1.02
CAM	0.6 [0.49–0.73]	10.4 [9.23–11.76]	27	0.36	5.3 [5.06–5.48]	–0.90

<sup>a</sup> The WT competition curve showed the best-fit to a single-site model. The mutant competition curves showed the best fit to a two-site model (Prism).



(Javitch et al., 1997) we found that MTSEA inhibited binding of [ $^3$ H]CGP-12177 up to around 40% in the D130N mutant, whereas concomitant mutation of Cys-285 (D130N/C285S) eliminated this inhibition (Fig. 8). Importantly, mutation of Cys-285 did not revert the constitutively activated phenotype of D130N as indicated by unchanged high affinity for the full agonist ISO. In competition binding experiments with [ $^3$ H]CGP-12177 on membranes from HEK 293 cells, a  $K_i$  value for ISO of  $1.52 \pm 0.37$  nM (mean  $\pm$  S.E.,  $n = 3$ ) was

observed for D130N and  $1.52 \pm 0.35$  nM for D130N/C285S (mean  $\pm$  S.E.,  $n = 3$ ). Furthermore, both D130N and D130N/C285S displayed the same affinity for [ $^3$ H]CGP-12177 ( $K_d$  [D130N] =  $55 \pm 2$  pM,  $K_d$  [D130N/C285S] =  $78 \pm 18$  pM, means  $\pm$  S.E.,  $n = 3$ ).

## Discussion

In this study, we sought to investigate the functional significance of the conserved Asp-130<sup>3.49</sup> (Fig. 1) in the DRY motif at the bottom of TM 3 in the  $\beta_2$ AR. Our data provide

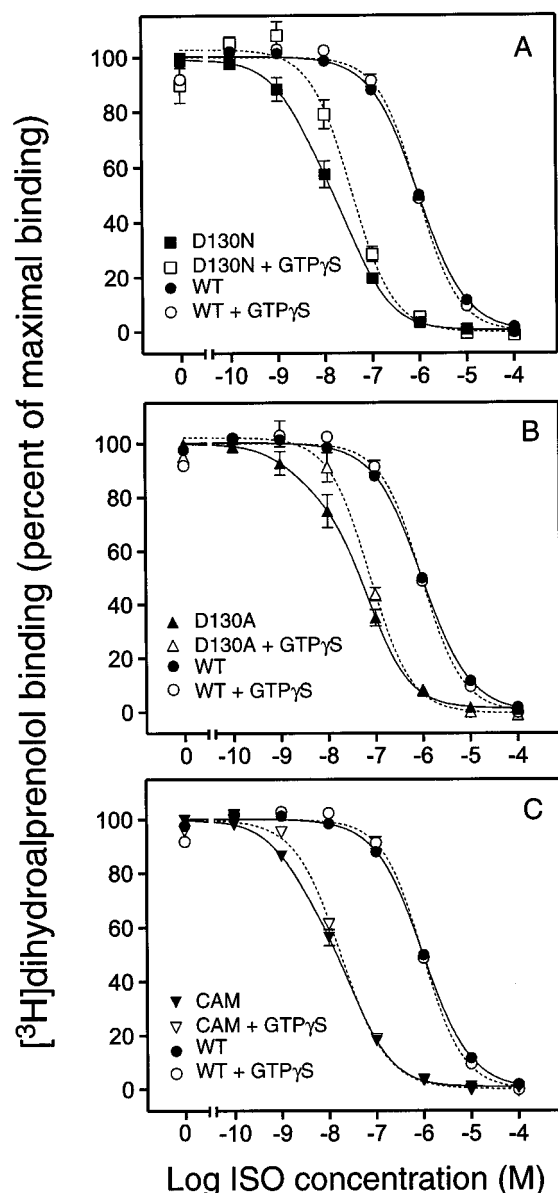


**Fig. 6.** ISO competition binding isotherms in the absence and presence of GTP $\gamma$ S. A, ISO competition of [ $^3$ H]dihydroalprenolol binding at D130N in absence (■, solid curve) or presence (□, short-dashed curve) of GTP $\gamma$ S. B, ISO competition of [ $^3$ H]dihydroalprenolol binding at D130A in absence (▲, solid curve) or presence (△, short-dashed curve) of GTP $\gamma$ S. C, ISO competition of [ $^3$ H]dihydroalprenolol binding at CAM in absence (▼, solid curve) or presence (▽, short-dashed curve) of GTP $\gamma$ S. ISO competition of [ $^3$ H]dihydroalprenolol binding at the WT receptor in absence (●, solid curve) or presence (○, short-dashed curve) of GTP $\gamma$ S is shown for comparison in all three panels. Data are the percentage of maximum [ $^3$ H]dihydroalprenolol binding (mean  $\pm$  S.E.,  $n = 3-5$ ). The experiments were done in COS-7 cell membranes prepared as described in *Experimental Procedures*.

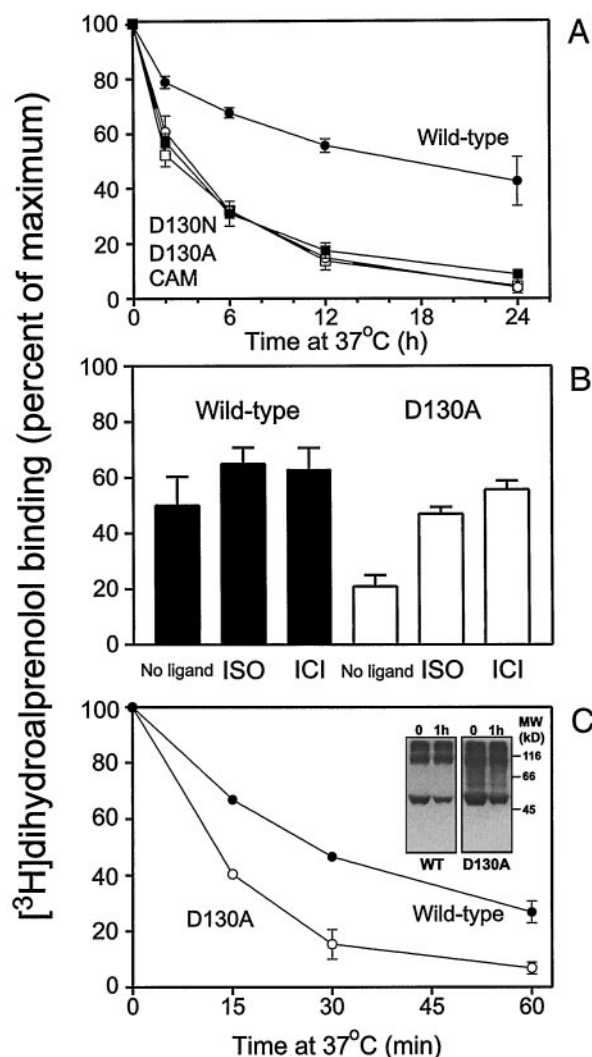


**Fig. 7.** Structural instability of D130N, D130A, and CAM. A, stability of WT and mutant receptors transiently expressed in COS-7 cells. Membranes expressing WT (●), D130N (■), D130A (○), or CAM (□) were incubated at 37°C for indicated periods of time. The remaining [ $^3$ H]dihydroalprenolol binding activity is given as a percentage of control at  $T = 0$  (mean  $\pm$  S.E.,  $n = 3$ ). B, effect of ligands on receptor stability. COS-7 cell membranes expressing WT or D130A were incubated for 6 h at 37°C in the absence or presence of 10  $\mu$ M (—)ISO or 1  $\mu$ M ICI 118,551. Data are remaining [ $^3$ H]dihydroalprenolol binding activity in the percentage of control at  $T = 0$  (mean  $\pm$  S.E.,  $n = 3$ ). C, stability of partially purified receptors from Sf-9 insect cells. Nickel chromatography purified WT (●) and D130A (○) were incubated at 37°C for indicated periods of time. The remaining [ $^3$ H]dihydroalprenolol binding activity is given as a percentage of control at  $T = 0$  (mean  $\pm$  S.E.,  $n = 3$ ). Inset, Western blot analysis of nickel-purified WT and D130A before and after incubation at 37°C for 60 min. The same amount of receptor as determined by initial binding activity was applied to the gel (0.2 pmol).

several lines of evidence that this aspartic acid plays a key role in the receptor activation mechanism. Interestingly, mutation of Asp-130<sup>3,49</sup> to D130N in the  $\beta$ 2AR has been reported previously (Fraser et al., 1988). In agreement with our results, an increase in agonist affinity without change in antagonist affinity was observed. However, no basal activity of either the WT or the mutant receptors was reported. Furthermore, agonist-promoted increase in cAMP production for the mutant receptor was not detected (Fraser et al., 1988). Most likely, the low expression of the mutant in B82 cells (42 fmol/mg protein), as compared with the much higher expression we obtain in COS-7, hindered detection of functional coupling and thus a relative increase in coupling efficiency (Fraser et al., 1988).

The DRY motif (Fig. 1) is highly conserved throughout the subfamily of rhodopsin-like GPCRs. Whereas the arginine (Arg-131<sup>3,50</sup>) is 100% conserved, the aspartic/glutamic acid (Asp-130<sup>3,49</sup>) is conserved among 99% of GPCRs belonging to rhodopsin-like receptors and the tyrosine (Tyr-132<sup>3,51</sup>) among approximately 75% of the receptors (Probst et al., 1992). Mutation of the arginine has established an important role of this residue in G protein activation (Min et al., 1993; Rosenthal et al., 1993; Scheer et al., 1996; Ballesteros et al., 1998). Previous studies have also indicated a critical function of Asp-130<sup>3,49</sup> for receptor activation. Charge-neutralizing mutations of the aspartic acid lead to constitutive activation of the adrenergic  $\alpha_{1b}$  receptor and improved coupling of the

GnRH receptor (Ballesteros et al., 1998). In the M1 muscarinic receptor mutation of the aspartic acid leads to phosphoinositide turnover responses quantitatively similar to the WT despite dramatically lowered expression (Lu et al., 1997). In rhodopsin, mutation of the corresponding glutamic acid causes weak constitutive receptor activation, and experiments have indicated that proton uptake by the glutamic acid is an important event in formation of metarhodopsin II (Cohen et al., 1993; Arnis et al., 1994).

The mutational data have been supported by molecular modeling and computational simulations. Based on simulations in the  $\alpha_{1B}$  receptor, Scheer et al. (1996) suggested that the Arg3.50 in the inactive state is constrained in a "polar pocket" formed by residues in TMs 1, 2, and 7. Upon protonation (or mutation) of the adjacent Asp3.49 (Asp-130) the arginine shifts out of the polar pocket leading to long range conformational changes. The ionic counterpart of the arginine in the inactive state was predicted to be the conserved aspartic acid in TM 2 (Asp2.50; Asp-79 in  $\beta$ 2AR, Fig. 1; Scheer et al., 1996). Alternatively, based on computational simulations in the GnRH receptor, Ballesteros et al. (1998) proposed that the ionic counterpart of Arg3.50 in the inactive state could be the adjacent Asp3.49 and not Asp2.50. They hypothesized that during receptor activation, Asp3.49 becomes protonated and that Asp2.50 substitutes for Asp3.49 in forming an ionic interaction with Arg3.50. Thus, an ionic interaction between Arg3.50 and Asp2.50 was associated with the active state instead of with the inactive state as proposed by Scheer et al. (1996) and Ballesteros et al., (1998). Nevertheless, both the model proposed by Scheer et al. (1996) and by Ballesteros et al. (1998) are in full agreement with our results and both underline that Asp3.50 (Asp-130) has a key role in receptor activation.

To assess the conformational state of the receptor after mutation of Asp-130, we utilized an assay based on the accessibility of an endogenous cysteine in TM 6 of the  $\beta$ 2AR (Cys285<sup>6,47</sup>) to a charged sulfhydryl specific reagent, MTSEA. Reaction with MTSEA covalently couples  $\text{SCH}_2\text{CH}_2\text{NH}_3^+$  to the cysteine sulfhydryl (Stauffer and Karlin, 1994). Methanethiosulfonate derivatives such as MTSEA react more than a billion times faster with the thiolate anion than with the thiol, and only water-accessible cysteines are likely to ionize to a significant extent (Roberts et al., 1986). The binding site of the  $\beta$ 2AR and homologous receptors for small water-soluble agonists is contained within a water-accessible binding-site crevice formed by the seven membrane-spanning segments (Javitch et al., 1995, 1997). Accordingly, a cysteine facing the water-accessible binding-site crevice should react much faster with charged MTSEA than should a cysteine facing the lipid bilayer or another membrane-spanning segment. As illustrated in Fig. 8, we provide evidence that Cys285<sup>6,47</sup> becomes partially accessible to MTSEA in the binding-site crevice in response to the mutation of Asp-130 to D130N. Our functional data strongly suggest that D130N spontaneously assumes an activated state, thus, the increased accessibility of Cys-285<sup>6,47</sup> most likely reflects a conformational change involved in receptor activation. A similar increase in the accessibility of Cys-285<sup>6,47</sup> was observed in CAM (Javitch et al., 1997). Importantly, the fact that similar changes in the accessibility of Cys-285<sup>6,47</sup> are seen with constitutively activating mutations both in TM 3 and in TM 6 suggests that the increased accessibility is a general function of activation,

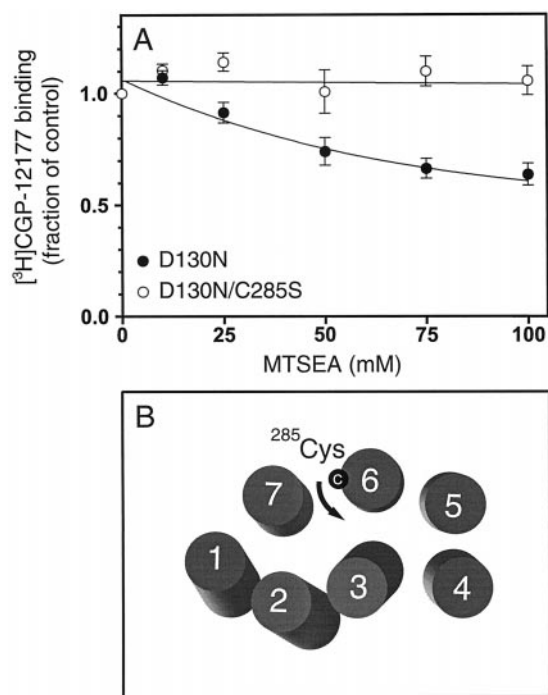


**Fig. 8.** Effects of MTSEA treatment on specific [ $^3\text{H}$ ]CGP-12177 binding to D130N and D130N/C285S. A, HEK 293 cells transiently expressing D130N (●) or D130N/C285S (○) were treated with indicated concentrations of MTSEA before determination of specific [ $^3\text{H}$ ]CGP-12177 binding. The data are given as a fraction of control binding activity without MTSEA treatment (means  $\pm$  S.E.,  $n = 3$ ). B, model of the seven TMs of the human  $\beta$ 2AR as seen from the extracellular side based on the projection structure of rhodopsin (Ballesteros and Weinstein, 1995; Baldwin et al., 1997). The suggested rearrangement of TM 6 in the activated state of the receptor (counterclockwise rotation or tilting) brings Cys-285<sup>6,47</sup> to the margin of the binding crevice where it becomes partially accessible to MTSEA.



and not simply a local structural change resulting from the mutation of residues at the bottom of TM 6.

According to a model of the  $\beta_2$ AR, Cys-285<sup>6,47</sup> is pointing toward TM 7 and is located in a boundary zone between the lipid bilayer and the water-accessible binding crevice (Ballesteros and Weinstein, 1995; Baldwin et al., 1997; Fig. 8). The data are thus mostly consistent with a counterclockwise rotation (as seen from the extracellular side) or tilting of TM 6 in the activated state, bringing Cys-285<sup>6,47</sup> more toward the margin of the binding crevice. A similar movement is predicted both from EPR spectroscopy analyses in rhodopsin (Farrens et al., 1996) and from fluorescence spectroscopy analyses of agonist-induced conformational changes in the  $\beta_2$ AR (Gether et al., 1997b). Of interest, a rhodopsin mutant in which the glutamic acid corresponding to Asp-130<sup>3,49</sup> in the  $\beta_2$ AR was mutated to glutamine was recently analyzed by EPR spectroscopy (Kim et al., 1997). The analysis showed a partial activated conformation in the dark state in agreement with a weak constitutive activity of this rhodopsin mutant (Kim et al., 1997). Surprisingly, they detected only minor spectroscopic changes in the region corresponding to TM 6. However, the studies were performed on rhodopsin, i.e., in presence of 11-*cis*-retinal, which has the properties of an inverse agonist (Han et al., 1997). This may have prevented a full conversion of the receptor to the active state.

Recently we reported that the constitutively activated  $\beta_2$ AR, CAM (Samama et al., 1993), is characterized by structural instability of the receptor (Gether et al., 1997a). Furthermore, fluorescence spectroscopy analysis of CAM labeled with an environmentally sensitive cysteine-reactive fluorophore showed evidence for enhanced conformational flexibility as compared with the WT (Gether et al., 1997a). Due to low expression of the Asp-130<sup>3,50</sup> mutants in Sf-9 insect cells, we did not succeed in purifying sufficient receptor for spectroscopy. However, as shown in Fig. 7, we could demonstrate that mutation of Asp-130<sup>3,50</sup> in TM 3 did confer a similar structural instability to the receptor as observed for CAM. The data suggest that stabilizing conformational constraints have been disrupted both in CAM and in the Asp-130<sup>3,50</sup> mutants, providing indirect structural evidence for the concept that GPCRs are maintained preferentially in an inactive configuration by a network of stabilizing, intramolecular interactions. This was originally proposed by Kjelsberg et al. (1992), who observed that any amino acid substitution of Ala293<sup>6,34</sup> in the  $\alpha_{1B}$  receptor resulted in constitutive receptor activation. The concept has, for example, also been supported by the proposed presence of interhelical salt bridge constraints that are disrupted during receptor activation in the  $\alpha_{1B}$  receptor (Porter et al., 1996).

Receptor models based on the projection map of rhodopsin predict that Asp-130<sup>3,50</sup> at the bottom of TM 3 would be close to the four residues substituted in CAM at the bottom of TM 6 (L266S/K267R/H269K/L272A; Ballesteros and Weinstein, 1995; Baldwin et al., 1997). Thus, it is likely that mutation/protonation of Asp-130<sup>3,50</sup> or mutation of the four residues in CAM, directly or indirectly, may cause a similar conformational perturbation in this region. This is specifically supported by molecular dynamics simulations in the  $\alpha_{1B}$  receptor of the constitutively active mutant, A293E (Ala6.34 corresponding to Leu-272 in the  $\beta_2$ AR; Scheer et al., 1996). These simulations indicated conformational changes in this receptor mutant similar to the changes observed by analyzing

the protonated state of Asp3.50 or the Asp-to-Ala mutation of this residue (Scheer et al., 1996). This further emphasizes the importance of the cytoplasmic ends of TMs 3 and 6 as a critical switch region controlling activation of rhodopsin-like GPCRs.

## References

- Arnis S, Fahmy K, Hofmann KP and Sakmar TP (1994) A conserved carboxylic acid group mediates light-dependent proton uptake and signaling by rhodopsin. *J Biol Chem* **269**:23879–23881.
- Baldwin JM, Schertler GF and Unger VM (1997) An alpha-carbon template for the transmembrane helices in the rhodopsin family of G-protein-coupled receptors. *J Mol Biol* **272**:144–164.
- Ballesteros J, Kitanovic S, Guarnieri F, Davies P, Fromme BJ, Konvicka K, Chi L, Millar RP, Davidson JS, Weinstein H and Sealfon SC (1998) Functional microdomains in G-protein-coupled receptors. The conserved arginine-cage motif in the gonadotropin-releasing hormone receptor. *J Biol Chem* **273**:10445–10453.
- Ballesteros JA and Weinstein H (1995) Integrated methods for the construction of three-dimensional models and computational probing of structure-function relations in G protein coupled receptors. *Methods Neurosci* **25**:366–428.
- Chidiac P, Hebert TE, Valiquette M, Dennis M and Bouvier M (1994) Inverse agonist activity of beta-adrenergic antagonists. *Mol Pharmacol* **45**:490–499.
- Cohen GB, Yang T, Robinson PR and Oprian DD (1993) Constitutive activation of opsin: Influence of charge at position 134 and size at position 296. *Biochemistry* **32**:6111–6115.
- Farrens DL, Altenbach C, Yang K, Hubbell WL and Khorana HG (1996) Requirement of rigid-body motion of transmembrane helices for light activation of rhodopsin. *Science (Wash DC)* **274**:768–770.
- Fraser CM, Chung FZ, Wang CD and Venter JC (1988) Site-directed mutagenesis of human beta-adrenergic receptors: Substitution of aspartic acid-130 by asparagine produces a receptor with high-affinity agonist binding that is uncoupled from adenylate cyclase. *Proc Natl Acad Sci USA* **85**:5478–5482.
- Gether U, Ballesteros JA, Seifert R, Sanders-Bush E, Weinstein H and Kobilka BK (1997a) Structural instability of a constitutively active G protein-coupled receptor. Agonist-independent activation due to conformational flexibility. *J Biol Chem* **272**:2587–2590.
- Gether U and Kobilka BK (1998) G protein-coupled receptors. II. Mechanism of agonist activation. *J Biol Chem* **273**:17979–17982.
- Gether U, Lin S, Ghanouni P, Ballesteros JA, Weinstein H and Kobilka BK (1997b) Agonists induce conformational changes in transmembrane domains III and VI of the beta2 adrenoceptor. *EMBO J* **16**:6737–6747.
- Gether U, Lin S and Kobilka BK (1995) Fluorescent labeling of purified beta2-adrenergic receptor: Evidence for ligand-specific conformational changes. *J Biol Chem* **270**:28268–28275.
- Guan XM, Kobilka TS and Kobilka BK (1992) Enhancement of membrane insertion and function in a type IIb membrane protein following introduction of a cleavable signal peptide. *J Biol Chem* **267**:21995–21998.
- Han M, Lou J, Nakanishi K, Sakmar TP and Smith SO (1997) Partial agonist activity of 11-*cis*-retinal in rhodopsin mutants. *J Biol Chem* **272**:23081–23085.
- Hjorth SA, Orskov C and Schwartz TW (1998) Constitutive activity of glucagon receptor mutants. *Mol Endocrinol* **12**:78–86.
- Javitch JA, Fu D, Chen J and Karlin A (1995) Mapping the binding-site crevice of the dopamine D2 receptor by the substituted-cysteine accessibility method. *Neuron* **14**:825–831.
- Javitch JA, Fu D, Liapakis G and Chen J (1997) Constitutive activation of the beta2 adrenergic receptor alters the orientation of its sixth membrane-spanning segment. *J Biol Chem* **272**:18546–18549.
- Javitch JA, Li X, Kaback J and Karlin A (1994) A cysteine residue in the third membrane-spanning segment of the human D2 dopamine receptor is exposed in the binding-site crevice. *Proc Natl Acad Sci USA* **91**:10355–10359.
- Ji TH, Grossmann M and Ji I (1998) G protein-coupled receptors. I. Diversity of receptor-ligand interactions. *J Biol Chem* **273**:17299–17302.
- Johansen TE, Scholler MS, Tolstoy S and Schwartz TW (1990) Biosynthesis of peptide precursors and protease inhibitors using new constitutive and inducible eukaryotic expression vectors. *FEBS Lett* **267**:289–294.
- Kim JM, Altenbach C, Thurmond RL, Khorana HG and Hubbell WL (1997) Structure and function in rhodopsin: Rhodopsin mutants with a neutral amino acid at E134 have a partially activated conformation in the dark state. *Proc Natl Acad Sci USA* **94**:14273–14278.
- Kjelsberg MA, Cotecchia S, Ostrowski J, Caron MG and Lefkowitz RJ (1992) Constitutive activation of the alpha 1b-adrenergic receptor by all amino acid substitutions at a single site. Evidence for a region which constrains receptor activation. *J Biol Chem* **267**:1430–1433.
- Lu ZL, Curtis CA, Jones PG, Pavia J and Hulme EC (1997) The role of the aspartate-arginine-tyrosine triad in the m1 muscarinic receptor: Mutations of aspartate 122 and tyrosine 124 decrease receptor expression but do not abolish signaling. *Mol Pharmacol* **51**:234–241.
- Min KC, Zvyaga TA, Cypess AM and Sakmar TP (1993) Characterization of mutant rhodopsins responsible for autosomal dominant retinitis pigmentosa. Mutations on the cytoplasmic surface affect transducin activation. *J Biol Chem* **268**:9400–9404.
- Porter JE, Hwa J and Perez DM (1996) Activation of the alpha1b-adrenergic receptor is initiated by disruption of an interhelical salt bridge constraint. *J Biol Chem* **271**:28318–28323.
- Probst WC, Snyder LA, Schuster DI, Brosius J and Sealfon SC (1992) Sequence alignment of the G-protein coupled receptor superfamily. *DNA Cell Biol* **11**:1–20.

- Roberts DD, Lewis SD, Ballou DP, Olson ST and Shafer JA (1986) Reactivity of small thiolate anions and cysteine-25 in papain toward methyl methanethiosulfonate. *Biochemistry* **25**:5595–5601.
- Rosenthal W, Antaramian A, Gilbert S and Birnbaumer M (1993) Nephrogenic diabetes insipidus. A V2 vasopressin receptor unable to stimulate adenylyl cyclase. *J Biol Chem* **268**:13030–13033.
- Salomon Y, Londos C and Rodbell M (1974) A highly sensitive adenylyl cyclase assay. *Anal Biochem* **58**:541–548.
- Samama P, Cotecchia S, Costa T and Lefkowitz RJ (1993) A mutation-induced activated state of the beta2-adrenergic receptor: Extending the ternary complex model. *J Biol Chem* **268**:4625–4636.
- Scheer A, Fanelli F, Costa T, De Benedetti PG and Cotecchia S (1996) Constitutively active mutants of the alpha 1B-adrenergic receptor: Role of highly conserved polar amino acids in receptor activation. *EMBO J* **15**:3566–3578.
- Scheer A, Fanelli F, Costa T, De Benedetti PG and Cotecchia S (1997) The activation process of the alpha1B-adrenergic receptor: Potential role of protonation and hydrophobicity of a highly conserved aspartate. *Proc Natl Acad Sci USA* **94**:808–813.
- Sheikh SP, Zvyaga TA, Lichtarge O, Sakmar TP and Bourne HR (1996) Rhodopsin activation blocked by metal-ion-binding sites linking transmembrane helices C and F. *Nature (Lond)* **383**:347–350.

- Schertler GF, Villa C and Henderson R (1993) Projection structure of rhodopsin. *Nature (Lond)* **362**:770–772.
- Stauffer DA and Karlin A (1994) Electrostatic potential of the acetylcholine binding sites in the nicotinic receptor probed by reactions of binding-site cysteines with charged methanethiosulfonates. *Biochemistry* **33**:6840–6849.
- Strader CD, Fong TM, Tota MR, Underwood D and Dixon RAF (1994) Structure and function of G protein-coupled receptors. *Annu Rev Biochem* **63**:101–132.
- Suryanarayana S and Kobilka BK (1991) Construction and expression of chimeric receptors to understand the structure-function relationships in adrenergic receptors. *Methods (Orlando)* **3**:193–204.
- Unger VM, Hargrave PA, Baldwin JM and Schertler GF (1997) Arrangement of rhodopsin transmembrane alpha-helices. *Nature (Lond)* **389**:203–206.
- Yu H, Kono M, McKee TD and Oprian DD (1995) A general method for mapping tertiary contacts between amino acid residues in membrane-embedded proteins. *Biochemistry* **34**:14963–14969.

---

**Send reprint requests to:** Dr. Ulrik Gether, Division of Cellular and Molecular Physiology, Department of Medical Physiology 12–5–22, The Panum Institute, University of Copenhagen, DK-2200 Copenhagen N, Denmark. E-mail: gether@mfi.ku.dk

---